Marine and Petroleum Geology 27 (2010) 1765–1774

Contents lists available at ScienceDirect

Marine and Petroleum Geology

journal homepage: www.elsevier.com/locate/marpetgeo

Petrophysical properties of bioclastic platform carbonates: implications for porosity controls during burial

Delphine Croizé [a,*], Stephen N. Ehrenberg [b], Knut Bjørlykke [a], François Renard [c], Jens Jahren [a]

[a] Department of Geosciences, University of Oslo, P.O. Box 1047, Blindern, N-0316 Oslo, Norway
[b] Oil and Gas Research Center, Sultan Qaboos University, Muscat, Sultanate of Oman
[c] LGCA-CNRS-Observatoire de Grenoble, Université Joseph Fourier BP 53, F-38041 Grenoble, France & Physics of Geological Processes, University of Oslo, Norway

ARTICLE INFO

Article history:
Received 15 December 2008
Received in revised form
17 September 2009
Accepted 19 November 2009
Available online 27 November 2009

Keywords:
Carbonate
Compaction
Triaxial tests
Porosity
Early diagenesis
Petrophysical properties
Acoustic velocity

ABSTRACT

This study is based on rock mechanical tests of samples from platform carbonate strata to document their petrophysical properties and determine their potential for porosity loss by mechanical compaction. Sixteen core-plug samples, including eleven limestones and five dolostones, from Miocene carbonate platforms on the Marion Plateau, offshore northeast Australia, were tested at vertical effective stress, σ_1', of 0–70 MPa, as lateral strain was kept equal to zero. The samples were deposited as bioclastic facies in platform-top settings having paleo-water depths of <10–90 m. They were variably cemented with low-Mg calcite and five of the samples were dolomitized before burial to present depths of 39–635 m below sea floor with porosities of 8–46%. Ten samples tested under dry conditions had up to 0.22% strain at $\sigma_1' = 50$ MPa, whereas six samples tested saturated with brine, under drained conditions, had up to 0.33% strain. The yield strength was reached in five of the plugs. The measured strains show an overall positive correlation with porosity. V_p ranges from 3640 to 5660 m/s and V_s from 1840 to 3530 m/s. Poisson coefficient is 0.20–0.33 and Young's modulus at 30 MPa ranged between 5 and 40 GPa. Water saturated samples had lower shear moduli and slightly higher P- to S-wave velocity ratios. Creep at constant stress was observed only in samples affected by pore collapse, indicating propagation of microcracks. Although deposited as loose carbonate sand and mud, the studied carbonates acquired reef-like petrophysical properties by early calcite and dolomite cementation. The small strains observed experimentally at 50 MPa indicate that little mechanical compaction would occur at deeper burial. However, as these rocks are unlikely to preserve their present high porosities to 4–5 km depth, further porosity loss would proceed mainly by chemical compaction and cementation.

1. Introduction

Shallow water carbonates are strongly affected by early diagenesis (Friedman, 1964). Widely variable early diagenetic processes affecting carbonate sediments make application of quantitative models for petrophysical properties more difficult than for siliciclastic rocks which are more stable at low temperature (Anselmetti and Eberli, 1993, 2001; Eberli et al., 2003; Adam et al., 2006; Vanorio et al., 2008). In large part because of varying early diagenesis, the Marion Plateau carbonate platforms display a wide range of petrophysical properties within a narrow range of depths (Isern et al., 2002; Ehrenberg et al., 2003, 2006c). They are therefore well suited for studying the impact of early diagenesis on mechanical compaction. Early carbonate diagenetic processes include dissolution of aragonite and magnesian calcite, precipitation of low-Mg calcite, as well as dolomitization (Meyers and Hill, 1983; Scholle and Halley, 1985). These processes can both add and remove large volumes of material, such that subsequent mechanical compaction during the first several hundred meters of burial depends strongly on the early diagenetic history (Hamilton, 1976; Scholle and Halley, 1985; Bassinot et al., 1993; Wallace et al., 2002). Although initial porosities of carbonate sediments are very high ranging around 50–60% (Enos and Sawatsky, 1981; Kroenke et al., 1991), porosities of subsurface carbonate reservoirs are generally much lower than in sandstones and commonly show trends of regular decrease as burial increases (Schmoker, 1984; Brown, 1997; Ehrenberg and Nadeau, 2005). At depth less than 2–2.5 km, i.e., temperature lower than 70–90 °C, mechanical compaction is commonly the main process of porosity loss in sandstones (Bjørlykke and Høeg, 1997; Paxton et al., 2002), but its importance in carbonates is more difficult to evaluate because of the irregular grain shapes and extensive diagenetic alteration characteristic of many carbonate sediments. Laboratory experiments

* Corresponding author.
E-mail address: delphine.croize@geo.uio.no (D. Croizé).

0264-8172/$ – see front matter © 2009 Elsevier Ltd. All rights reserved.
doi:10.1016/j.marpetgeo.2009.11.008

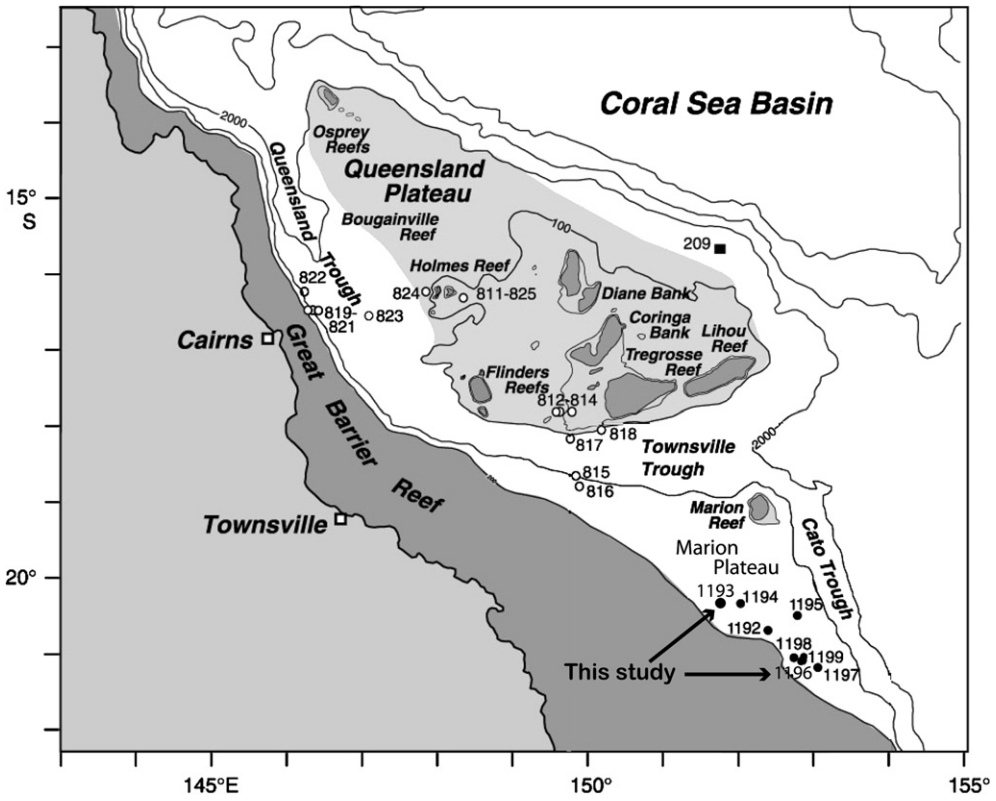

Fig. 1. Location of ODP drilling sites 1193 and 1196 where the tested samples were taken (modified from Isern et al. (2002)).

showed that when carbonates are not cemented, mechanical compaction plays a major role on porosity loss (Goldhammer, 1997; Chuhan et al., 2003). While carbonate rocks are mostly studied based on outcrop or cores from reservoirs, the present study measures the petrophysical properties of Miocene carbonate rocks buried at 39–635 m below sea floor which represents their maximal burial depth. The results provide a basis for predicting porosity at greater depth and understanding the respective roles of mechanical and chemical compaction in carbonate sediments.

2. Samples

The samples studied are from two Miocene carbonate platforms that were cored during Ocean Drilling Program (ODP) Leg 194 on the Marion Plateau, just seaward of the Great Barrier Reef on the northeastern Australian continental margin (Pigram et al., 1992; Isern et al., 2002). These cores are characterized by strong petrophysical heterogeneities over short vertical depth intervals, reflecting varying influence of both depositional textures and diagenesis (Ehrenberg et al., 2006b). Details regarding the units sampled and the separation of the samples into different textural classes are provided by Isern et al. (2002); Ehrenberg et al. (2006a). Fifteen horizontally oriented, 25 mm core-plugs were selected among the samples analysed by Ehrenberg et al. (2003) (Figs. 1 and 2). One additional sample, plug 1.2, is a vertically oriented plug drilled from whole-core sample EHWR1 (Ehrenberg, 2007). The samples consist of eleven limestones and five dolostones cored from depth of 39–365 m below sea floor. The sediments were deposited as loose bioclastic grains and mud in paleo-water depths estimated to have been less than 10 to less than 100 m (Isern et al., 2002). Principal bioclasts are large benthic foraminifers, red algae and bryozoans. Plugs have porosities of 8–46% and permeabilities ranging from 0.04 to >50 000 mD (Table 1). A wide scatter is observed in the permeability – porosity relationship and no clear relationship between textures and porosity – permeability trends is apparent (Fig. 3). Comparison between plug and whole-core measurements for the Marion Plateau samples shows that plug samples, despite their smaller size, adequately represent the petrophysical properties of the studied cores (Ehrenberg, 2007). The sixteen samples selected for testing include nine plugs from site 1193, penetrating the Northern Marion Platform (NMP) and seven plugs from site 1196, on the Southern Marion Platform (SMP) (Table 1). The samples include

Fig. 2. Plugs 18, 21, 22 and 30 before compaction.

Table 1
Sample characteristics, test conditions and calculated elastic parameters.

site[a]	plug	z[b]	mineralogy	tex[c]	GD[d]	height[e]	k[f]	Φ[g]	conditions	σ'_{1ini}[h]	σ'_{3ini}[h]	σ'_{1final}[h]	E[i]	ν[i]	K[i]	μ[i]	β[i]	V_p[j]	V_s[j]
1193	18	45.97	Limestone	O	2.71	21.00	213.0	20.2	Dry	1.66	0.5	50	19.6	0.25	19.7	16.3	3.34	3927	2454
1196	69	56.97	Dolostone		2.82	21.43	1014.0	27.0	Dry	1.66	0.5	50	22.1	0.24	21.1	17.9	3.98	4081	2526
1193	21	63.74	Limestone	C	2.71	25.10	8835.0	26.4	Dry	1.25	0.5	50	19.5	0.23	11.0	20.8	4.42	3833	2774
1193	22	67.92	Limestone	X	2.72	23.60	1.18	17.6	Dry	1.66	0.5	50	21.9	0.28	11.4	23.53	2.90	4028	2899
1193	30	73.79	Limestone	O	2.70	29.25	3236.0	18.2	Dry	1.25	0.5	50	28.5	0.26	20.5	21.7	2.43	4359	2803
1196	114	316.86	Limestone	F	2.71	22.50	0.18	12.8	Dry	5	2	50	30.2	0.24	28.0	18.9	2.54	4523	2652
1196	160	539.35	Dolostone		2.73	26.27	0.04	8.4	Dry	1.25	0.5	30	33.3	0.33	39.8	35.9	1.30	5630	3542
1196	167	557.51	Dolostone		2.82	27.73	5545.0	31.5	Dry	1.25	0.5	30	20.9	0.24	28.6	17.1	3.69	4292	2497
1196	201	633.88	Dolostone		2.76	23.15	12.60	15.3	Dry	9.8	2.94	50	30.9	0.23	36.0	23.5	1.81	4934	2937
1196	203	634.98	Dolostone		2.78	21.67	4094.0	26.5	Dry	9.8	2.94	50	18.1	0.20	29.9	13.5	3.85	4129	2198
1196	1.2	38.58	Limestone	X	2.75	19.54	1.3	25.0	Saturated	1.66	0.5	70	8.63	0.30	29.7	15.3	11.7	4358	2355
1193	2	42.16	Limestone	O	2.70	22.54	22 314	17.4	Saturated	1.66	0.5	70	14.9	0.27	41.1	19.3	3.57	5008	2678
1193	4	43.19	Limestone	O	2.68	19.35	2169	16.0	Saturated	1.66	0.5	70	12.4	0.29	32.3	16.3	3.60	4495	2485
1193	17	45.69	Limestone	O	2.72	21.60	325	24.7	Saturated	1.66	0.5	70	8.56	0.25	35.5	15.4	6.38	4550	2366
1193	52	61.34	Limestone	C	2.72	17.46	6.31	18.3	Saturated	1.66	0.5	50	14.2	0.26	29.1	14.3	3.84	4191	2271
1193	31	74.16	Limestone	C	2.70	24.24	> 50 000	46.0	Saturated	1.66	0.5	7					18.8	4264	2463

[a] ODP drilling site number.
[b] Depth in meters below sea floor.
[c] Texture: C = coarse grainstone, F = fine grainstone, X = packstone with isolated vugs, O = packstone with large vugs (From Ehrenberg et al., 2006a).
[d] Grain density (g/cm^3).
[e] Plug height (mm).
[f] Klinkenberg-corrected gas permeability (mD).
[g] Porosity (%).
[h] Initial and final stress values during triaxials tests (MPa).
[i] Elastic parameters calculated at $\sigma'_1 = 30$ MPa: E = Young's Modulus (GPa), ν = Poisson ratio, K = bulk modulus (GPa), μ = shear modulus (GPa), β = compressibility (10^{-11} Pa^{-1}).
[j] Acoustic velocity in meters per second, mean values measured at $\sigma'_1 = 20$ MPa (Except for plug 31 for which σ'_1 is less than 10 MPa).

eleven limestones and five dolostones, meaning that they contain 80% or more calcite or dolomite, respectively. All samples originally had bioclastic textures (packstone, grainstone, floatstone) and have negligible siliciclastic content.

3. Experimental method

3.1. K0 triaxial tests

The experimental method used is K_0 triaxial testing under drained conditions. K_0 stands for coefficient of lateral stress at rest, $K_0 = \sigma'_3/\sigma'_1$, where σ'_3 is horizontal effective stress and σ'_1 is vertical effective stress, both are expressed in MPa. The samples are cylindrical plugs of about 25 mm in diameter and 17–29 mm in height. All plugs were ground at top and bottom to make the two end surfaces plane and parallel. For some plugs plaster was added on the end surfaces to fill large pores and ensure an uniform application of load on the surface. Plaster was also applied at a few places on the sample sides to prevent the confining membrane from being pressed into cavities and thereby being punctured at high cell pressures. The plugs were then dried at 50–60 °C. Two knobs were glued, diametrically opposed, at the middle height of the sample for fixation of the radial deformation sensor. The samples were then sprayed with latex rubber to create a confining membrane.

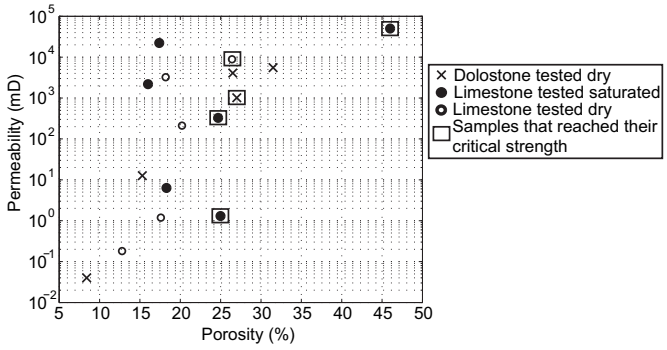

Fig. 3. Permeability versus porosity (Actual values are to be found in Table 1).

The samples were mounted into the triaxial cell and subjected to a vacuum of about 0.1 MPa inside the confining membrane and then subjected to a confining pressure of about 0.5 MPa. The vacuum was then released by allowing air into the sample for the dry tests and brine for the saturated tests. For the saturated tests a back pressure of 5 MPa was applied by increasing confining pressure and pore pressure simultaneously to 5.5 and 5.0 MPa, respectively, to secure good saturation. The effective stresses were then increased to σ'_{1ini} and σ'_{3ini} values given in Table 1. Then vertical stress was increased at a rate of 3.75 MPa per hour for the dry tests and 5 MPa per hour for the saturated tests to the σ'_{1final} values given in Table 1, while strain in the horizontal direction was prevented by continuously adjusting the lateral stress. The effective vertical stress was calculated from the measurements of the effective confining pressure and the deviator load applied by piston through the top of the cell and measured by the internal load cell. The pressure controllers (for cell and pore pressure) and the loading press (for deviator load) were connected to a PC so that the stresses could be applied automatically. Deformations were recorded by two vertical LVDT deformation sensors and one radial LVDT deformation sensor. Considering the experimental method and accounting for false deformation, vertical deformation readings were estimated to be accurate to about ±0.002 mm. The brine used to saturate the plugs consisted of 35 g dissolved NaCl per litre water. Tangent Young's modulus, E, and Poisson ratio, ν, were calculated at 30 MPa from stress and strain measurements (Table 1). The following relations were used to determine ν (eq. (1)) and E (eq. (2)) from stress and vertical strain, ε_1 (Turcotte and Schubert, 1982):

$$\nu = \frac{\sigma'_3}{\sigma'_1 + \sigma'_3}; \tag{1}$$

$$E = \frac{\sigma'_1 \cdot (1+\nu) \cdot (1-2\nu)}{(1-\nu) \cdot \varepsilon_1}. \quad (2)$$

3.2. Acoustic velocity measurement

Compressional and shear wave velocities were measured throughout the tests at regular time intervals using the pulse transmission technique (Birch, 1960). P- and S-wave piezoelectric transducers were mounted inside the base and top plates of the triaxial cell to measure P- and S-wave velocities along the plug axis. Resonant frequency of the crystals was, according to the manufacturer, 500 kHz. Compressional and shear wave velocities measured are between 3640 and 5660 and 1840–3530 m/s, respectively. Although the resonant frequency of the glued crystal may deviate somewhat from the one of the pure crystal, the wavelength of the ultrasonic pulse is assumed to range from 3.7 to 11.3 mm, which is less than the plugs radius. This arrangement is assumed to be sufficient to avoid diffraction phenomena and unwanted shape mode. The signals were recorded on a computer, and first arrival times picked manually. At low stresses, S-wave first arrivals are difficult to pick, but the clarity of the signal improves as effective vertical stress increases. Correction for equipment was applied to the P- and S-wave velocities. First arrival times, t_0, were measured with no sample in between the base and top plates. This zero time was then subtracted from the picked traveltime, t_s, measured with a plug present. The plug's compressional or shear wave velocity was then calculated as: $V_{p/s} = h_s/(t_s - t_0)$, where h_s is the height of the sample. Bulk and shear modulus were calculated at 30 MPa from V_p and V_s measurements.

4. Results

4.1. Stress–strain relationship

From the stress–strain curves (Fig. 4) most of the deformation is interpreted to be linear elastic. The saturated tests show greater compressibility than the dry tests (Figs. 4 and 5). At $\sigma'_1 = 50$ MPa, the vertical strain, ε_1, is less than 0.22% for the dry tests, while ε_1 is greater than 0.22% for the saturated tests (Fig. 4a, b). The critical strength, i.e., the stress value where failure or gradual yielding starts, of the plugs was reached for two samples during the dry tests and three samples during the saturated tests (Fig. 4c, d). For plug 1.2, at vertical effective stress greater than 35 MPa, the stress–strain relation is non-linear possibly indicating start of strain hardening. These five samples exhibiting the onset of failure or gradual yielding all have high porosity relative to the other samples (Fig. 5), suggesting that rock strength may be related to the degree of cementation. Compressibility, $\beta = \Delta\varepsilon/\Delta\sigma'_1$, was calculated for dry and wet experiments. Compressibility of the dry plugs, β_{dry}, is 1.30–4.42·10^{-11} Pa^{-1} and compressibility of the saturated plugs, β_{sat}, is 3.57–18.8·10^{-11} Pa^{-1} (Fig. 5). Compressibility correlates with porosity in both groups. Comparison with published data for dry compressibility of carbonates (Bell, 1981;

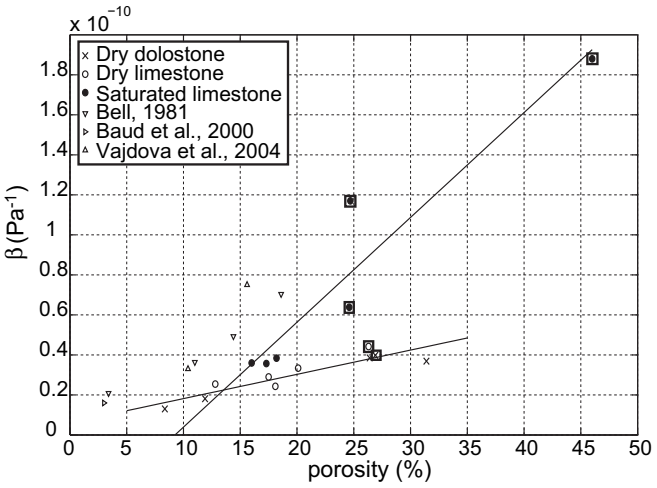

Fig. 5. Compressibility versus porosity, comparing present results with published data. Samples that reached their yield strength are enclosed in black square. The lines correspond to best linear fit for dry and wet samples.

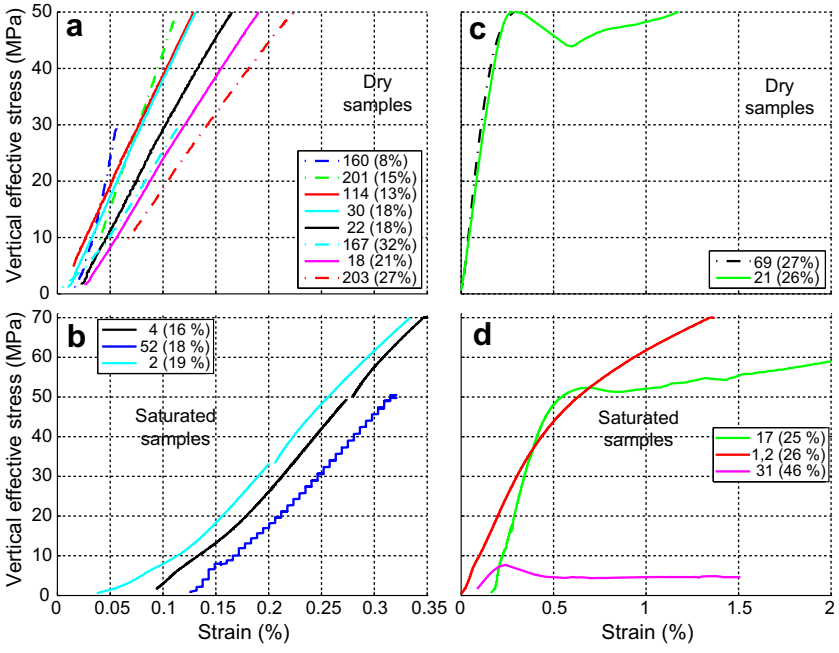

Fig. 4. Effective stress versus strain. Line pattern indicates mineralogy, dashed lines = dolostone and solid lines = Limestone. Sample porosity is shown in parentheses.

Baud et al., 2000; Vajdova et al., 2004) shows that present samples are less compressible for a given porosity (Fig. 5). The non-linear part of the stress–strain curves at low stresses is inferred to be due to closure of cracks (Baud et al., 2000).

Young's moduli are between 5 and 40 GPa and Poisson's ratios are in the range 0.2–0.33 (Fig. 6 and Table 1). The studied samples display a more or less linear relation between horizontal and vertical effective stresses. This implies that Poisson's ratio remains almost constant during the tests, showing only minor decrease with increasing stress (Fig. 6). A dramatic decrease of E with increasing stress is observed for sample 21, 69, 17, 1.2 and 31, this is interpreted as the beginning of brittle deformations.

Both for dry and saturated samples, Young's modulus decreases with increasing porosity (Fig. 6). Dry limestones of the present study have lower Young's moduli than found in those studied by Palchik and Hatzor (2002), this is especially noticeable at low porosities (Fig. 6). Calculations by the modified Mori - Tanaka's relationship (Luo and Weng, 1987), using elastic constants of calcite (Bhimasenachar, 1945) and dolomite (Nur and Simmons, 1969), give higher values of both Young's modulus and Poisson ratio than the experimental data (Fig. 6). Lack of correlation between E or ν and porosity most likely indicates that others factors, such as pore shape and texture, play an important role in determining the mechanical strength of carbonates.

Creep was observed in the five samples in which the critical strength was reached (Fig. 7), whereas no creep occurred in the plugs that did not reach their critical strength. Failure was, most likely, followed by crack propagation and volume reduction, which could also be an effective means of mechanical compaction.

4.2. Acoustic velocities

P and S-wave velocities show little increase with stress, which should be expected since strain values are small (Fig. 8). Compressional velocities increase slightly at low stress, but become approximately constant above $\sigma'_1 = 10$ MPa, this is more pronounced for low velocity samples (Fig. 8). The velocity increase is in agreement with the non linearity of the stress – strain curves at low stresses which may be related to the closure of cracks (Fortin et al., 2007). At similar porosities, higher compressional velocities are observed in saturated than in dry conditions (Fig. 8), in agreement with previous studies (Winkler and Nur, 1979; Yale, 1985; Tao et al., 1995; Adam et al., 2006).

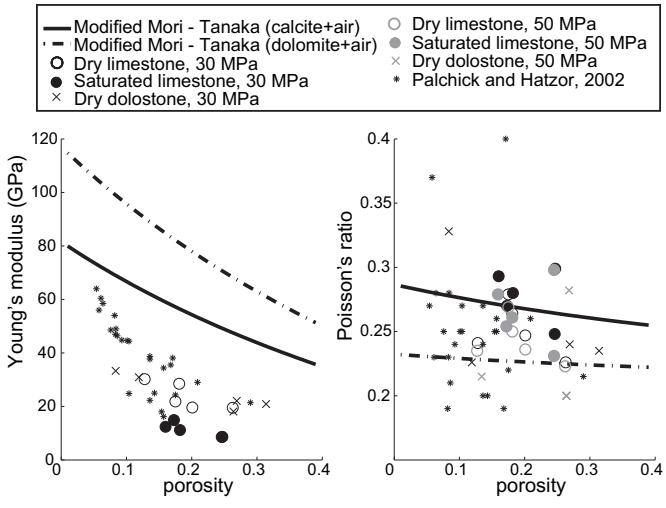

Fig. 6. Young modulus and Poisson's ratio at σ_1' of 30 and 50 MPa versus porosity. Present results are compared with data of Palchik and Hatzor (2002) and values calculated by the modified Mori - Tanaka's method (Luo and Weng, 1987).

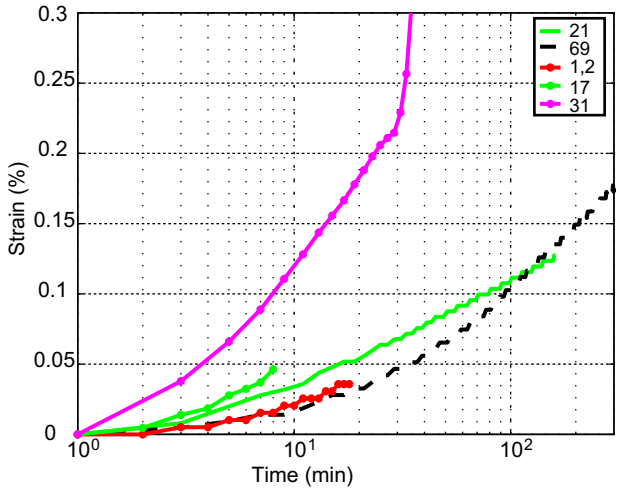

Fig. 7. Creep at constant stress of plugs 69 and 21 at 50 MPa, plugs 1.2 and 17 at 70 MPa and plug 31 at 4.6 MPa.

Wide ranges of V_p and V_s values are observed in the present samples, with the lowest velocities occurring in the samples showing greatest strains (Figs. 4 and 8). The high variability of V_p and V_s within a narrow depth range is similar to the variability observed in samples from the Great Bahama Bank (Anselmetti and Eberli, 2001). The samples with the lowest porosity have as expected (Verwer et al., 2008) the highest V_p (Fig. 10). Scatter in the V_p values might be due to variations in types of cement (Eberli et al., 2003), and pore geometry (Tao et al., 1995; Dürrast and Siegesmund, 1999; Sayers, 2008; Verwer et al., 2008). V_p–V_s ratio is constant during tests and tends to be higher in the saturated plugs. V_p/V_s is 1.39–1.87 for dry samples and 1.80–1.95 for saturated samples (Fig. 9).

Bulk and shear modulus calculated from V_p and V_s measurements are plotted together with Hashin - Shtrikman bounds in Fig. 11. Bulk modulus data are well predicted by theory. Two limestones samples and one dolostone sample have higher shear modulus than the Hashin - Shtrikman upper bound (Fig. 11). Dolostones have slightly higher bulk modulus, while shear modulus does not seem to be influenced by mineralogy. The saturated tests have overall lower shear modulus than the dry tests, but there are too few data to be certain (Fig. 11). Such an effect is not predicted by Gassmann (1951), but has been noted in previous carbonate studies (Baechle et al., 2005; Vanorio et al., 2008).

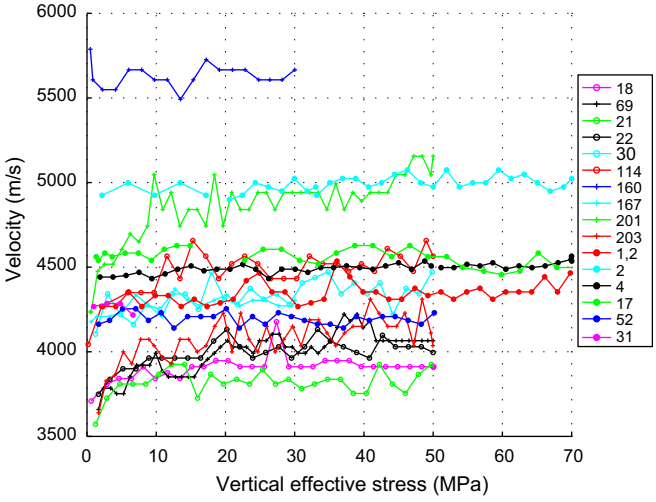

Fig. 8. P-wave velocity versus vertical effective stress for all samples.

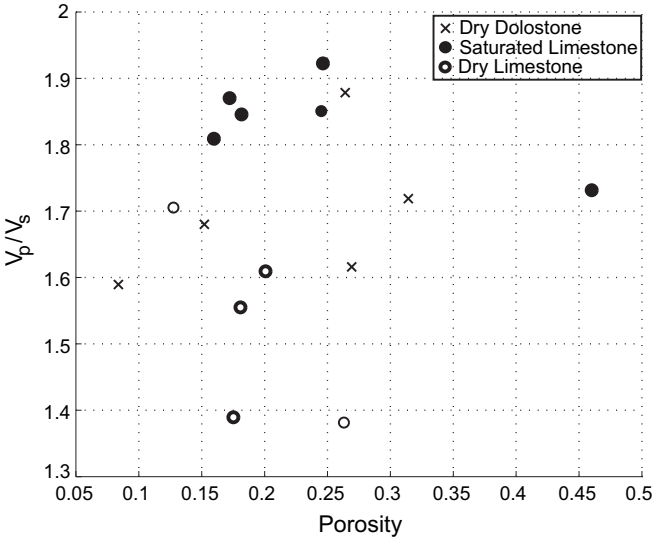

Fig. 9. Vp to Vs ratio versus porosity. Vp to Vs ratios were calculated with mean values of Vp and Vs at vertical stress greater than 20 MPa. Plug 31 ($\Phi = 46\%$) reached its critical strength at 7 MPa, therefore for this plug Vp–Vs ratio was calculated from values at vertical stress below 7 MPa.

4.3. Relationship between microstructures and physical properties

Two features common to all the limestone samples are dominance of bioclasts and cementation by low-Mg calcite (plug 52, 18 Fig. 12). Dolostone samples were also constituted mainly of bioclasts, but have been replaced and cemented by dolomite.

Of the five plugs that reached their critical strength, samples 21 and 31 have pore diameters larger than encountered in most other tested plugs (see Table 2). The observation of Chuhan et al. (2003) that coarse-grained sediments are more compressible than fine grained sediments may explain the greater compaction shown by sample 1.2 which contains larger grains than other samples (Fig. 12). Sample 69 is cemented by micro-crystals of dolomite that have precipitated homogeneously inside the matrix, creating pores with a wide range of shapes and providing many sites for cracks nucleation and propagation. Sample 17 contains abundant microporosity,

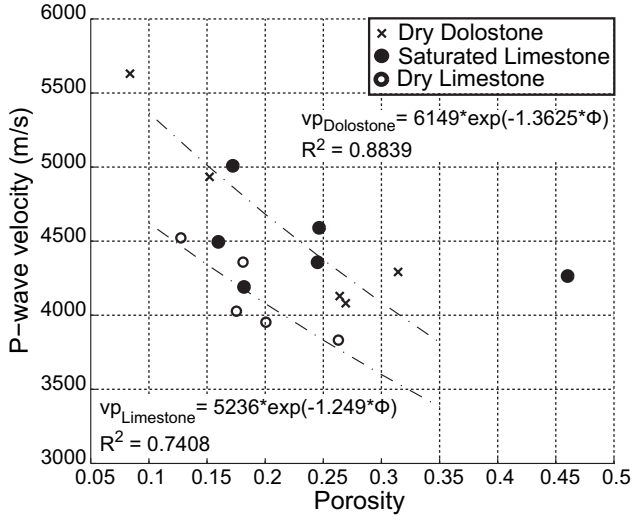

Fig. 10. Vp at 30 MPa versus porosity. Best fits for limestone and dolostone are displayed, no good fit was found for saturated samples.

in addition to larger pores, and inter-granular and intra-granular microcracks. Coalescence of microcracks after compression tests was observed in samples 1.2 and 17 (Fig. 12).

The aspect ratio of pores (long axis divided by short axis) was measured on thin section photographs (Table 2). The data show that brittle behaviour is associated with higher values of pore aspect ratio for given porosity (Fig. 13). At comparable porosity, larger pores (Table 2) are associated with increased likelihood of failure. This can perhaps be explained by assuming that smaller pore sizes result from higher cement contents and consequent increase in rock strength.

Plug 4 and 52 have lower velocity than the other water saturated samples (Fig. 10). Plug 4 has a high pore aspect ratio (Table 2), which may explain its low compressional velocity (Baechle et al., 2005; Adam et al., 2006; Vanorio et al., 2008). However this explanation is not valid for plug 52. Therefore, in the present study, the scatter in acoustic velocity is not explained by changes in pore size and shape only.

5. Discussion

Eleven of the sixteen plug tested displayed a linear stress–strain relationship. Among those plugs, little mechanical compaction was obtained during K_0 triaxial tests at vertical effective stress up to 70 MPa (Fig. 4). These Marion Plateau carbonates are less compressible than carbonates with lower porosity tested in other studies. Triaxial tests on dry Solnhofen, Indiana and Tavel limestones with porosities ranging from 3 to 13%, showed strains ranging from 0.19 to 0.46% at confining pressure of 50 MPa (Vajdova et al., 2004). Dry tests on the Marion Plateau plugs show maximum strain at $\sigma'_1 = 50$ MPa of 0.22% while on average they are more porous than the carbonates studied by Vajdova et al. (2004) (Fig. 4). The lower compressibility of the Marion Plateau samples than other cemented limestones (Bell, 1981; Baud et al., 2000; Vajdova et al., 2004) is tentatively attributed to greater cementation of the former. The present study suggests that cementation has made the Marion Plateau carbonates stronger than would be expected from their porosity and depth values, resulting in only minor porosity reduction in response to the stresses applied. Although the above comparisons concern specifically limestones, the Marion Plateau dry dolostones do not display different stress–strain relationship than the dry limestones. The formation of a stable framework built during early diagenesis, makes these samples stronger than expected from porosity and depth values. Increasing applied stress on these samples produced little porosity reduction, therefore for these type of rocks mechanical compaction is not the main process of porosity reduction with burial.

The hypothesis of strength correlating with amount and, possibly, types of cementation can be tested by measuring the samples by modal analysis, i.e., point counting, of thin sections. These data are not part of the existing dataset, but are planned to be acquired, now that the probable role of cementation has been identified.

During K_0 tests, the plugs walls are prevented from collapsing by the regulation of the lateral stress. This is also prevented in sedimentary basins due to lateral stresses exerted by surrounding sediments. Nevertheless, five of the sixteen plugs reached their critical strength during testing (Fig. 4). For the saturated samples, the three limestones out of six that reached their critical strength, all have porosities greater than 20%. Among the saturated samples, three different textures are represented, one of each reached its critical strength. For the dry tests, two out of ten plugs failed, both having porosity greater than 20%, although three other samples with porosity greater than 20% did not fail. One common feature of the two dry samples that reached their yield strength is the

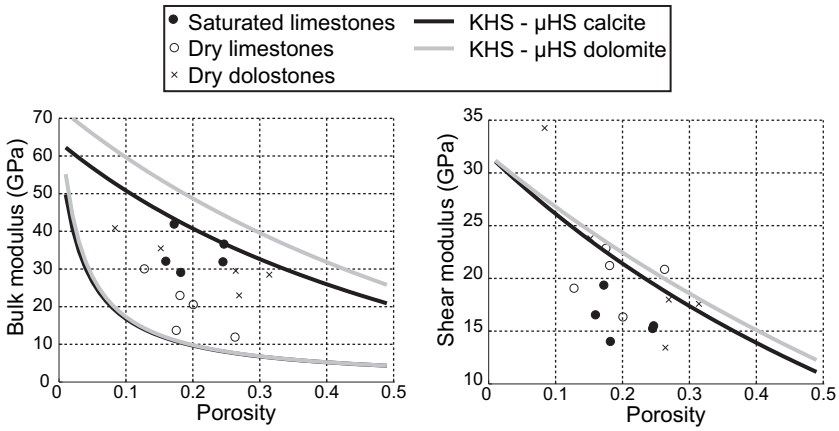

Fig. 11. Shear and bulk modulus at 30 MPa, calculated from V_p and V_s values, versus porosity. Hashin - Shtrikman upper and lower bounds for bulk, *KHS*, and shear, *μHS*, modulus were calculated for calcite and dolomite, the pores being filled by air.

combination of high pore aspect ratio and high porosity (Fig. 13, Table 2). Failure seems to be most likely occurring in coarse-grained samples than in fine grained ones, although this is not true in all cases. Different factors may decide on competence versus failure of these samples, but the present study clearly shows that high porosity is favourable to failure, as no failure occurred in samples with porosity less than 20% (Fig. 5).

Only the data for limestones can be compared between dry and saturated states because the dolomite were only tested dry. The saturated limestones show much greater increase in compressibility at higher porosities than dry samples, such that $\beta_{sat}-\beta_{dry}$ increases with porosity (Fig. 5). However, the compressibility–porosity correlation is much stronger for the dry samples. As expected from the compressibility results, the saturated limestones have lower elastic moduli than the dry limestones (Fig. 6). Another effect of saturation is that shear moduli values are lower and bulk moduli tend to be higher in saturated samples (Fig. 11). The dry limestone and dolostone data define two parallel velocity–porosity trends (Fig. 10), whereas no trend is apparent for the saturated samples. Higher V_p–V_s ratios are also found in saturated limestones (Fig. 9).

Young's modulus tends to decrease with increasing porosity as predicted by theory (Fig. 6), even though the predicted values are

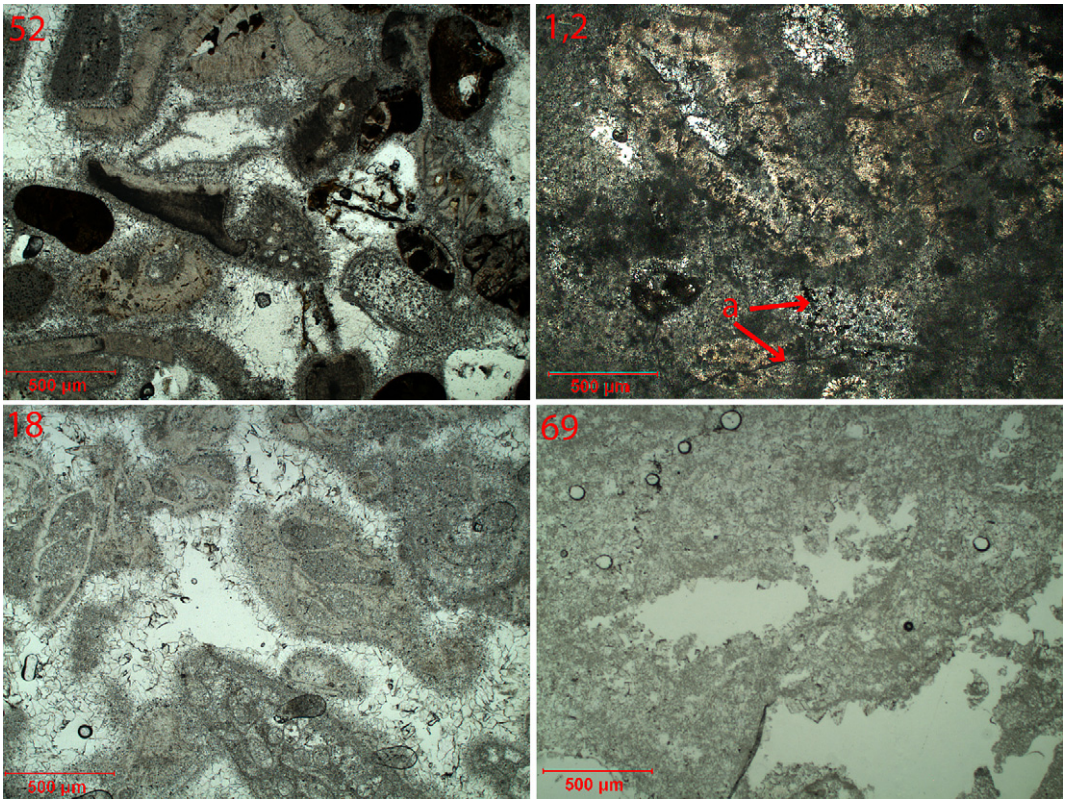

Fig. 12. Thin sections of samples 52, 1.2, 18 and 69 before triaxial test showing the heterogeneity of grain sizes and pore shapes. Samples 52 and 18 did not break, because sparitic cement reinforced the pores, forming vault like structures that could sustain the stress. Samples 1.2 (a: cracks propagation) and 69 (no cement did reinforce the pores) did show a brittle behaviour at 50 MPa.

Table 2
Mean values of the pore size and aspect ratio, and their dispersion.

Plug	N[a]	Mean((a+b)/2)[b]	Var((a+b)/2)[c]	Mean(AR)[d]	Var(AR)[c]
18	40	0.25	0.053	2.7	2.2
69	54	0.19	0.171	2.6	1.2
21	40	0.35	0.100	3.5	6.2
22	32	0.16	0.012	2.1	0.6
30	40	0.32	0.109	2.2	1.2
114	47	0.08	0.003	2.5	7.7
160	41	0.24	0.083	1.9	0.3
167	57	0.24	0.020	2.0	0.8
201	45	0.22	0.025	1.9	1.2
203	49	0.29	0.028	2.1	0.6
1.2	18	0.21	0.012	2.2	1.4
2	35	0.36	0.139	2.6	1.6
4	28	0.22	0.016	2.8	2.7
17	38	0.16	0.013	2.5	2
52	39	0.18	0.012	2.1	1.7
31	35	0.57	0.171	2.4	1.2

[a] N = number of pores measured.
[b] a = long axis of the pores (mm), b = small axis of the pores (mm).
[c] var = variance.
[d] AR = Pore aspect ratio, AR = a/b.

higher than the measured values. Young's modulus values obtained during this study are in agreement with values obtained on limestones by Palchik and Hatzor (2002). As expected from the compressibility results, the saturated samples have lower elastic moduli than the dry samples (Fig. 6). Porosity is probably the main factor controlling compressibility and elasticity, but poor correlations between porosity and these mechanical properties indicates that other factors are also important. For the dry samples, bulk and shear moduli are higher in dolostones than in limestones at equivalent porosity values (Fig. 11, Table 1).

V_p ranges from 3640 to 5660 m/s and V_s from 1840 to 3530 m/s for the plugs of this study. Compressional velocities are lower than most published data for which $V_{pLimestone}$ ranges from 6200 to 6500 m/s, and $V_{pDolostone}$ from 6900 to 7400 m/s (Mavko et al., 1998). Dolostone and limestone do not display different stress–strain relationship (Fig. 5), but dolostone samples do have significantly higher ultrasonic velocity (Fig. 10). As noted above, the dry limestone and dolostone data define two parallel velocity–porosity trends (Fig. 10). The velocities values of this study are similar to those measured on samples of equivalent porosity and depth from the Great Bahamas Bank (Anselmetti and Eberli, 2001). The results of this study confirm a strong correlation of P-wave velocity with total porosity under dry conditions and variably higher velocities for given porosity in limestones under saturated conditions (Fig. 10). The minimal scatter in the dry data suggests that these samples may share basic similarities in pore geometry and matrix connectivity, as these factors are known to introduce scatter in velocity–porosity data (Anselmetti and Eberli, 2001). The considerably greater scatter in the saturated data in Fig. 10 can be better examined when petrographic analyses become available.

Vertical stress of 50 MPa is equivalent to approximately 4–5 km burial depth under hydrostatic fluid pressure. The K_0 tests thus simulate the potential natural burial of the Marion Plateau platforms to depths corresponding to the Earth's deeper petroleum reservoirs. The present experimental results indicate that increasing burial of the Marion Plateau carbonates can therefore be expected to result in two different types of behaviour:

1. The more strongly cemented samples will experience elastic deformation and little porosity loss by mechanical compaction (Fig. 4a,b).
2. The less cemented or more porous samples will fail by crack propagation (Fig. 7), breaking grain-to-grain contacts and allowing further porosity loss by mechanical compaction.

For the majority of the samples, the observation of very little compaction at stresses up to 50 MPa, indicates that almost no porosity reduction would occur by mechanical compaction if these rocks were buried at 4–5 km depth. Average porosity of the set of samples is about 20% and very little porosity loss is obtained during testing. It is unlikely that this amount of porosity would be preserved at 4–5 km burial depth. For example, Ehrenberg and Nadeau (2005) show that average porosity of carbonate petroleum reservoirs worldwide is around 8% at 4–5 km depth. We may therefore conclude that the porosity reduction in such strata occurs mainly by chemical processes as depth increases with burial. This implies that the rate of porosity loss is a function of dissolution and precipitation processes and is unrelated to mechanical compaction. For the subordinate population of weak samples with porosity greater than 20%, failure by crack propagation will cause local porosity loss.

The stratigraphic distribution of porosity in the two Marion Platform profiles, together with the tested sample locations, provides an indication of the locations prone to mechanical failure. As the failed samples are all from depths of less than 80 m below sea floor, it can be speculated that these weak intervals might become more strongly cemented and thus resistant to failure

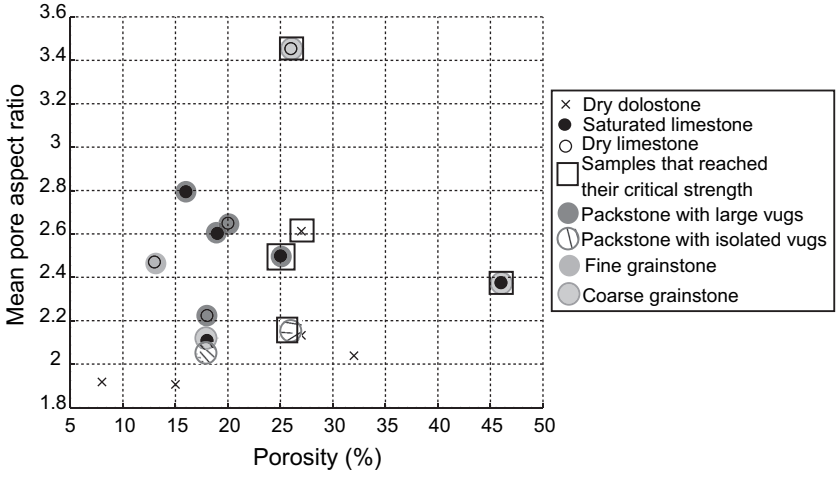

Fig. 13. Mean pore aspect ratio versus initial porosity.

before burial deeper than a few hundred meters. In such case, the conclusions derived from the non-failed samples may apply to the entire section of each platform.

6. Conclusions

- In this study, total porosity and early cementation are identified as fundamental controls on carbonate rock strength and compressibility, as well as on other parameters like elastic moduli.
- Early cementation of bioclastic carbonate sediments has produced a stable cemented framework with a high degree of over-consolidation and low compressibility.
- The effect of water saturation was observed in both the weakening of the mechanical strength and greater scatter in the correlation of P-wave velocity versus porosity.
- Variation in mineralogy does not influence the compressibility of the plugs strongly, but acoustic velocities of dolostones are systematically higher than in limestones.
- Most of the present carbonate sediments were already so strongly cemented at 30–400 m that further porosity loss during burial to to 4–5 km depth must occur mainly by chemical rather than mechanical processes. The more porous samples, however, would respond to increased burial by failure due to crack propagation.

Acknowledgements

Samples used were provided by the Ocean Drilling Program, which is sponsored by the U.S. National Science Foundation and participating countries under management of Joint Oceanographic Institutions, Inc. The authors would like to thank Toralv Berre, Trude Ørbech and Sven Vangbæk from the Norwegian Geotechnical Institute for their help in the laboratory and helpful comments on an earlier version of this manuscript. The two anonymous reviewers are also thanked for their constructive comments.

References

Adam, L., Batzle, M., Brevik, I., 2006. Gassmann's fluid substitution and shear modulus variability in carbonates at laboratory seismic and ultrasonic frequencies. Geophysics 71 (6), F173–F183.

Anselmetti, F.S., Eberli, G.P., 1993. Controls on sonic velocity in carbonates. Pure and Applied Geophysics 141 (2–4), 287–323.

Anselmetti, F.S., Eberli, G.P., 2001. Sonic velocity in carbonates - a combined product of depositional lithology and diagenetic alterations. In: Ginsburg, R. (Ed.), Subsurface Geology of a Prograding Carbonate Platform Margin, Great Bahama Bank: Results of the Bahamas Drilling Project. SEPM Special Publication, vol. 70, pp. 193–216.

Baechle, G.T., Weger, R.J., Eberli, G.P., Massaferro, J.L., Sun, Y.-F., 2005. Changes of shear moduli in carbonate rocks: implications for gassmann applicability. The Leading Edge 24 (5), 507–510.

Bassinot, F., Marsters, J., Mayer, L., Wilkens, R., 1993. Variations of porosity in calcareous sediments from the ontong java plateau. In: Kroenke, L.W., Berger, W.H., Janecek, T.R., et al. (Eds.), Proc. ODP, Sci. Results, vol. 130. Ocean Drilling Program, College Station, TX, pp. 653–661,. doi:10.2973/odp.proc.sr.130.058.1993.

Baud, P., Schubnel, A., Wong, T.F., 2000. Dilatancy, compaction, and failure mode in solnhofen limestone. Journal of Geophysical Research, B, Solid Earth and Planets 105 (8), 19,289–19,303.

Bell, F.G., 1981. A survey of the physical properties of some carbonate rocks. Bulletin of Engineering Geology and the Environment 24 (1), 105–110. doi:10.1007/BF02595261.

Bhimasenachar, J., 1945. Elastic constants of calcite and sodium nitrate. Proceeding of the Indian Acadamy of Scirnce Section A.

Birch, F., 1960. The velocity of compressional waves in rocks to 10 kilobars, part 1. Journal of Geophysical Research 65 (4), 1083–1102.

Bjørlykke, K., Høeg, K., 1997. Effects of burial diagenesis on stresses, compaction and fluid flow in sedimentary basins. Marine and Petroleum Geology 14 (3), 267–276.

Brown, A., 1997. Porosity variation in carbonates as a function of depth: mississippian madison group, williston basin. In: Kupecz, J., Gluyas, J., Bloch, S. (Eds.), Reservoir Quality Prediction in Sandstones and Carbonates: AAPG Memoir, vol. 69, pp. 29–46.

Chuhan, F.A., Kjeldstad, A., Bjørlykke, K., Høeg, K., 2003. Experimental compression of loose sands; relevance to porosity reduction during burial in sedimentary basins. Canadian Geotechnical Journal=Revue Canadienne de Geotechnique 40 (5), 995–1011.

Dürrast, H., Siegesmund, S., 1999. Correlation between rock fabrics and physical properties of carbonate reservoir rocks. International Journal of Earth Sciences 88 (3), 392–408.

Eberli, G.P., Baechle, G.T., Anselmetti, F.S., Incze, M.L., 2003. Factors controlling elastic properties in carbonate sediments and rocks. The Leading Edge 22 (7), 654–660.

Ehrenberg, S.N., 2007. Whole core versus plugs: scale dependence of porosity and permeability measurements in platform carbonates. AAPG Bulletin 91 (6), 835–846.

Ehrenberg, S.N., Eberli, G.P., Bracco, G.G.L., 2003. Data report: porosity and permeability of miocene carbonate platforms on the marion plateau, odp leg 194. In: Anselmetti Flavio, S., Isern Alexandra, R., Blum, P., et al. (Eds.), Proc. ODP, Sci. Results, vol. 194. Texas A&M University, Ocean Drilling Program, College Station, TX, United States, pp. 1–217,. doi:10.2973/odp.proc.sr.194.007.2004.

Ehrenberg, S.N., Eberli, G.P., Baechle, G.T., 2006a. Porosity–permeability relationships in miocene carbonate platforms and slopes seaward of the great barrier reef, australia (odp leg 194, marion plateau). Sedimentology 53 (6), 1289–1318.

Ehrenberg, S.N., Eberli, G.P., Keramati, M., Moallemi, S.A., 2006b. Porosity–permeability relationships in interlayered limestone–dolostone reservoirs. AAPG Bulletin 90 (1), 91–114.

Ehrenberg, S.N., McArthur, J.M., Thirlwall, M.F., 2006c. Growth, demise, and dolomitization of miocene carbonate platforms on the marion plateau, offshore ne australia. Journal of Sedimentary Research 76 (1), 91–116.

Ehrenberg, S.N., Nadeau, P.H., 2005. Sandstone vs. carbonate petroleum reservoirs; a global perspective on porosity - depth and porosity – permeability relationships. AAPG Bulletin 89 (4), 435–445.

Enos, P., Sawatsky, L.H., 1981. Pore networks in holocene carbonate sediments. Journal of Sedimentary Petrology 51 (3), 961–985.

Fortin, J., Gueguen, Y., Schubnel, A., 2007. Effects of pore collapse and grain crushing on ultrasonic velocities and v-p/v-s. Journal of Geophysical Research-Solid Earth 112 (B8).

Friedman, G.M., 1964. Early diagenesis and lithification in carbonate sediments. Journal of Sedimentary Research 34 (4), 777–813.

Gassmann, F., 1951. Elasticity of high-porosity sandstone: uber die elastizitat poroser medien. Vierteljahrsschr. Nat. Ges. Zurich 96, 1–23.

Goldhammer, R.K., 1997. Compaction and decompaction algorithms for sedimentary carbonates. Journal of Sedimentary Research 67 (1), 26–35.

Hamilton, E.L., 1976. Variations of density and porosity with depth in deep-sea sediments. Journal of Sedimentary Petrology 46 (2), 280–300.

Isern, A.R., Anselmetti, F.S., Blum, P., et al., 2002. Init. repts. In: Shipboard Scientific Party Proc. ODP, vol. 194. Ocean Drilling Program, College Station, TX, pp. 1–116,. doi:10.2973/odp.proc.ir.194.104.2002.

Kroenke, L.W., Berger, W.H., Janecek, T.R., et al., 1991. Proc.. Odp, Init. Repts. 130. doi:10.2973/odp.proc.ir.130.1991.

Luo, H.A., Weng, G.J., 1987. On eshelby inclusion problem in a 3-phase spherically concentric solid, and a modification of mori-tanakas method. Mechanics of Materials 6 (4), 347–361.

Mavko, G., Mukerji, T., Dvorkin, J., 1998. The Rock Physics Handbook: Tools for Seismic Analysis in Porous Media. Cambridge University Press, Cambridge.

Meyers, W.J., Hill, B.E., 1983. Quantitative studies of compaction in mississippian skeletal limestones, new mexico. Journal of Sedimentary Petrology 53 (1), 231–242.

Nur, A., Simmons, G., 1969. Effect of saturation on velocity in low porosity rocks. Earth and Planetary Science Letters 7 (2), 183–193.

Palchik, V., Hatzor, Y.H., 2002. Crack damage stress as a composite function of porosity and elastic matrix stiffness in dolomites and limestones. Engineering Geology 63 (3–4), 233–245.

Paxton, S.T., Szabo, J.O., Ajdukiewicz, J.M., Klimentidis, R.E., 2002. Construction of an intergranular volume compaction curve for evaluating and predicting compaction and porosity loss in rigid-grain sandstone reservoirs. AAPG Bulletin 86 (12), 2047–2067.

Pigram, C.J., Davies, P.J., Feary, D.A., Symonds, P.A., 1992. Absolute magnitude of the second-order middle to late miocene sea-level fall, marion plateau, northeast australia. Geology (Boulder) 20 (9), 858–862.

Sayers, C.M., 2008. The elastic properties of carbonates. The Leading Edge 27 (8), 1020–1024.

Schmoker, J.W., 1984. Empirical relation between carbonate porosity and thermal maturity - an approach to regional porosity prediction. Aapg Bulletin-American Association of Petroleum Geologists 68 (11), 1697–1703.

Scholle, P.A., Halley, R.B., 1985. Burial diagenesis; out of sight, out of mind! In: Schneidermann, N., Harris Paul, M. (Eds.), Carbonate Cements Special Publication - Society of Economic Paleontologists and Mineralogists. SEPM (Society for Sedimentary Geology), vol. 36. United States, Tulsa, OK, pp. 309–334.

Tao, G., King, M.S., Nabibidhendi, M., 1995. Ultrasonic wave-propagation in dry and brine-saturated sandstones as a function of effective stress - laboratory measurements and modeling. Geophysical Prospecting 43 (3), 299–327.

Turcotte, D.L., Schubert, G., 1982. Geodynamics; Applications of Continuum Physics to Geological Problems. John Wiley & Sons, New York, NY, United States.

Vajdova, V., Baud, P., Wongf, T., 2004. Compaction, dilatancy, and failure in porous carbonate rocks. Journal of Geophysical Research, B, Solid Earth and Planets 109, B05204.

Vanorio, T., Scotellaro, C., Mavko, G., 2008. The effect of chemical and physical processes on the acoustic properties of carbonate rocks. The Leading Edge 27 (8), 1040–1048.
Verwer, K., Braaksma, H., Kenter, J.A.M., 2008. Acoustic properties of carbonates: effects of rock texture and implications for fluid substitution. Geophysics 73 (2), B51–B65.
Wallace, M.W., Holdgate, G.R., Daniels, J., Gallagher, S.J., Smith, A., 2002. Sonic velocity, submarine canyons, and burial diagenesis in oligocene-holocene cool-water carbonates, gippsland basin, southeast australia. AAPG Bulletin 86 (9), 1593–1607.
Winkler, K., Nur, A., 1979. Pore fluids and seismic attenuation in rocks. Geophysical Research Letters 6 (1), 1–4.
Yale, D.P., 1985. Recent advances in rock physics. Geophysics 50 (12), 2480–2491.